AMCA Congreso Anual 2009 de la Asociación de México de Control Automático. Zacatecas, México.

Adaptive Control for 2D Visual Servoing

Juan C. Rivera, Maximiliano Bueno–López and Marco A. Arteaga †

***Abstract*— Visual servoing is a useful approach for robot control. It is specially attractive when the control objective can be stated directly in image coordinates like in point–to–point regulation. In this paper, we propose an adaptive control for a robot manipulator, which allows the displacement of the end-effector between two points previously known. For implementation requires joint, image coordinates and some parameters of the camera. It is assumed that the robot is planar and the camera fixed, so that the image plane is parallel to the manipulator workspace. Simulation results show the good performance of the complete system.**

Index Terms: Visual Servoing, robot control, Adaptive Control.

I. Introduction

The problem of designing adaptive control laws for rigid-robot manipulators that ensure asymptotic trajectory tracking has interested researchers for many years. The development of effective adaptive controllers represents an important step toward high-speed/precision robotic applications. Even in a well-structured industrial facility, robots may face uncertainty regarding the parameters describing the dynamic properties. Since the parameters are difficult to compute or measure, they limit the potential for robots to manipulate accurately objects of considerable size and weight. It has recently been recognized that the accuracy of conventional approaches in high-speed applications is greatly affected by parametric uncertainties. To compensate for this parametric uncertainty, many researches have proposed adaptive strategies for the control of robotic manipulators. Using Visual servoing and adaptive control, we look for to estimate a set of parameters more quickly and achieve the desired trajectory in less time.

The fixed camera strategy is a common approach in visual servoing for robot control. Usually, the objective consists in making the manipulator end–effector follow a specified trajectory or reach a final point in the workspace (Hutchinson et al., 1996). The resulting performance depends on many factors, among them the knowledge of camera parameters. In (Kelly et al., 2000) an alternative to camera calibration is proposed by carrying out vision system identification, while in (Dean et al., 2006) a control algorithm is introduced which effectively deals with an unknown environment to achieve not only position but also force control. On the other hand, a good performance does not depend only on knowing well the complete visual system and robot model. Recently, in (Arteaga et al., 2008) an algorithm is proposed based on velocity fields. Although no specialized approaches were employed to get camera and manipulator model parameters, the outcomes were good. The great benefit that can be obtained from using visual servoing is the accuracy that is obtained with a configuration in closed loop, which makes the system relatively insensitive to calibration errors. Thus, we introduce a point-to-point control using only image, joint coordinates and the focal length of the camera.

The paper is organized as follows: Section II gives the robot model and reviews the relationship between joint and image coordinates. The control approach is given in Section III, while the simulation results are presented in Section IV. Finally, some conclusions are given in Section V.

II. Preliminaries

The dynamics of a rigid robot arm with revolute joints can adequately be described by using the Euler–Lagrange equations of motion (Sciavicco et al., 2000), resulting in

$$\boldsymbol{H}(\boldsymbol{q})\ddot{\boldsymbol{q}} + \boldsymbol{C}(\boldsymbol{q},\dot{\boldsymbol{q}})\dot{\boldsymbol{q}} + \boldsymbol{D}\dot{\boldsymbol{q}} + \boldsymbol{g}(\boldsymbol{q}) = \boldsymbol{\tau} - \boldsymbol{\tau}_{\mathrm{p}}, \qquad (1)$$

where $\boldsymbol{q} \in \mathbb{R}^n$ is the vector of generalized joint coordinates, $\boldsymbol{H}(\boldsymbol{q}) \in \mathbb{R}^{n\times n}$ is the symmetric positive definite inertia matrix, $\boldsymbol{C}(\boldsymbol{q},\dot{\boldsymbol{q}})\dot{\boldsymbol{q}} \in \mathbb{R}^n$ is the vector of Coriolis and centrifugal torques, $\boldsymbol{g}(\boldsymbol{q}) \in \mathbb{R}^n$ is the vector of gravitational torques, $\boldsymbol{D} \in \mathbb{R}^{n\times n}$ is the positive semidefinite diagonal matrix accounting for joint viscous friction coefficients, $\boldsymbol{\tau} \in \mathbb{R}^n$ is the vector of torques acting at the joints, and $\boldsymbol{\tau}_{\mathrm{p}} \in \mathbb{R}^n$ represents any bounded external perturbation or friction force.

Let us denote the largest (smallest) eigenvalue of a matrix by $\lambda_{\max}(\cdot)$ ($\lambda_{\min}(\cdot)$). For a $n\times 1$ vector $\boldsymbol{x}$, we shall use the Euclidean norm $\|\boldsymbol{x}\| \triangleq \sqrt{\boldsymbol{x}^{\mathrm{T}}\boldsymbol{x}}$, while the norm of a $m \times n$ matrix $\boldsymbol{A}$ is the corresponding induced norm $\|\boldsymbol{A}\| \triangleq \sqrt{\lambda_{\max}(\boldsymbol{A}^{\mathrm{T}}\boldsymbol{A})}$. By recalling that revolute joints are considered, the following properties can be established:

Property 1: It holds $\lambda_{\mathrm{h}}\|\boldsymbol{x}\|^2 \leq \boldsymbol{x}^{\mathrm{T}}\boldsymbol{H}(\boldsymbol{q})\boldsymbol{x} \leq \lambda_{\mathrm{H}}\|\boldsymbol{x}\|^2$ $\forall\ \boldsymbol{q},\ \boldsymbol{x} \in \mathbb{R}^n$, and $0 < \lambda_{\mathrm{h}} \leq \lambda_{\mathrm{H}} < \infty$, given by

$$\lambda_{\mathrm{h}} \triangleq \min_{\forall \boldsymbol{q}\in\mathbb{R}^n} \lambda_{\min}(\boldsymbol{H}(\boldsymbol{q}))$$

$$\lambda_{\mathrm{H}} \triangleq \max_{\forall \boldsymbol{q}\in\mathbb{R}^n} \lambda_{\max}(\boldsymbol{H}(\boldsymbol{q})).$$

† J. C. Rivera, M. Bueno–López and M. A. Arteaga are with the Departamento de Control y Robótica. División de Ingeniería Eléctrica de la Facultad de Ingeniería. Universidad Nacional Autónoma de México. Apdo. Postal 70–256, México, D. F., 04510, México. Tel.: + 52 55–56–22–30–13. Fax: + 52 55–56–16–10–73. max@fi-b.unam.mx.

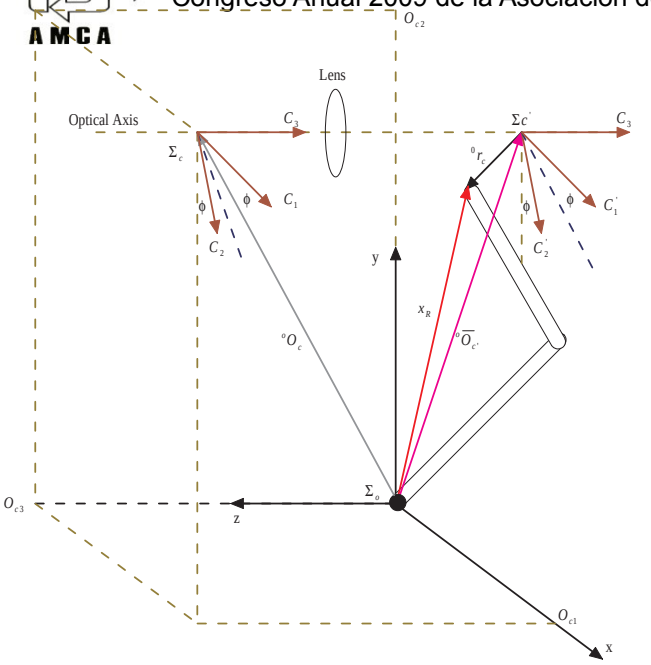

Figura 1. Reference System

Property 2: Using the Christoffel symbols (of the first kind) to compute $\boldsymbol{C}(\boldsymbol{q},\dot{\boldsymbol{q}})$, $\dot{\boldsymbol{H}}(\boldsymbol{q}) - 2\boldsymbol{C}(\boldsymbol{q},\dot{\boldsymbol{q}})$ is skew symmetric.

Throughout this paper, we will assume that the robot is a two degrees of freedom planar manipulator, *i. e.* we have $n = 2$ in eq. (1). Then, the direct kinematics is a differentiable map $\boldsymbol{f}_{\rm k}(\boldsymbol{q}) : \mathbb{R}^2 \to \mathbb{R}^2$

$$\boldsymbol{x}_{\rm R} = \boldsymbol{f}_{\rm k}(\boldsymbol{q}), \tag{2}$$

relating the joint positions $\boldsymbol{q} \in \mathbb{R}^2$ to the Cartesian position $\boldsymbol{x}_{\rm R} \in \mathbb{R}^2$ of the centroid of a target attached at the arm end–effector. On the other hand, the output variable of the robotic system is the position $\boldsymbol{y} \in \mathbb{R}^2$ of the image feature, *i. e.* the position of the target in the computer screen. In terms of the target position $\boldsymbol{x}_{\rm R}$ with respect to the robot base frame, the image feature $\boldsymbol{y}$ can be computed through transformation and a perspective projection as (Kelly et al., 2004). The workspace of the robot is shown in figure (1)

$$\begin{aligned} \boldsymbol{y} &= \frac{\alpha\lambda}{O^{\rm C}_{\rm R3} - \lambda}\boldsymbol{R}_\phi \left[\boldsymbol{x}_{\rm R} - \begin{bmatrix} O^{\rm C}_{\rm R1} \\ O^{\rm C}_{\rm R2} \end{bmatrix}\right] + \begin{bmatrix} u_{\rm o} \\ v_{\rm o} \end{bmatrix} \\ &\triangleq \alpha_\lambda \boldsymbol{R}_\phi \left[\boldsymbol{x}_{\rm R} - \begin{bmatrix} O^{\rm C}_{\rm R1} \\ O^{\rm C}_{\rm R2} \end{bmatrix}\right] + \begin{bmatrix} u_{\rm o} \\ v_{\rm o} \end{bmatrix}. \end{aligned} \tag{3}$$

$\boldsymbol{O}^{\rm C}_{\rm R} = [\, O^{\rm C}_{\rm R1} \quad O^{\rm C}_{\rm R2} \quad O^{\rm C}_{\rm R3} \,]^T$ is the position of the origin of the camera frame $\Sigma_{\rm C}$ with respect to the robot frame $\Sigma_{\rm R}$, λ is the focal length, α is a conversion factor from meters to pixels, and $[\, u_{\rm o} \quad v_{\rm o} \,]^{\rm T}$ is the center offset. We assume the camera image to be parallel to the robot plane of motion. $\boldsymbol{R}_\phi$ represents the orientation of the camera frame $\Sigma_{\rm C}$ with respect to the robot frame $\Sigma_{\rm R}$ and is given by

$$\boldsymbol{R}_\phi = \begin{bmatrix} \cos(\phi) & \sin(\phi) \\ \sin(\phi) & -\cos(\phi) \end{bmatrix}, \tag{4}$$

where $\phi \in \mathbb{R}$ is the angle of rotation. Note that $\boldsymbol{R}_\phi^{-1} = \boldsymbol{R}_\phi^{\rm T} = \boldsymbol{R}_\phi$. From (3) one gets the differential perceptual kinematic model given by

$$\dot{\boldsymbol{y}} = \alpha_\lambda \boldsymbol{R}_\phi \boldsymbol{J}(\boldsymbol{q})\dot{\boldsymbol{q}}, \tag{5}$$

where $\boldsymbol{J}(\boldsymbol{q}) = \partial \boldsymbol{f}_{\rm k}(\boldsymbol{q})/\partial \boldsymbol{q}$ is the so–called geometrical Jacobian matrix of the robot (Sciavicco et al., 2000), which satisfies the following well–known relationship

$$\dot{\boldsymbol{x}}_{\rm R} = \boldsymbol{J}(\boldsymbol{q})\dot{\boldsymbol{q}}. \tag{6}$$

Whenever the robot is not in a singularity, one also has the following relationship

$$\dot{\boldsymbol{q}} = \boldsymbol{J}^{-1}(\boldsymbol{q})\dot{\boldsymbol{x}}_{\rm R}. \tag{7}$$

Assumption 1: The robot does not reach any singularity.

III. Adaptive visual servoing control

In this section, a tracking controller based on image coordinates will be designed. The task to be accomplished by the robot is to go from its initial position $\boldsymbol{y}(0)$ to a final position $\boldsymbol{y}_{\rm f}$. To create a soft trajectory between these two points, we employ a polynomial of order 5. The tracking error in image coordinates is given by

$$\Delta\boldsymbol{y} \triangleq \boldsymbol{y} - \boldsymbol{y}_{\rm d}. \tag{8}$$

To design the tracking controller, let us define

$$\dot{\boldsymbol{y}}_{\rm r} = \dot{\boldsymbol{y}}_{\rm d} - \boldsymbol{\Lambda}_{\rm y}(\boldsymbol{y} - \boldsymbol{y}_{\rm d}) + \boldsymbol{s}_{\rm d} - \boldsymbol{K}_\gamma \boldsymbol{\sigma}, \tag{9}$$

where $\boldsymbol{K}_\gamma \in \mathbb{R}^{2\times 2}$ is a diagonal positive definite matrix and $\boldsymbol{\sigma} \in \mathbb{R}^2$, with

$$\boldsymbol{s} = \dot{\boldsymbol{y}} - \dot{\boldsymbol{y}}_{\rm d} + \boldsymbol{\Lambda}_{\rm y}(\boldsymbol{y} - \boldsymbol{y}_{\rm d}) \triangleq \dot{\tilde{\boldsymbol{y}}} + \boldsymbol{\Lambda}_{\rm y}\tilde{\boldsymbol{y}} \tag{10}$$

$$\boldsymbol{s}_1 = \boldsymbol{s} - \boldsymbol{s}_{\rm d} \tag{11}$$

$$\boldsymbol{s}_{\rm d} = \boldsymbol{s}(0)e^{-kt} \tag{12}$$

$$\boldsymbol{\sigma} = \int_0^t \{\boldsymbol{K}_\beta \boldsymbol{s}_1(\vartheta) + \mathrm{sign}(\boldsymbol{s}_1(\vartheta))\}\,\mathrm{d}\vartheta, \tag{13}$$

where $\boldsymbol{\sigma}(0) = \boldsymbol{0}$, k is a positive constant, $\boldsymbol{K}_\beta \in \mathbb{R}^{2\times 2}$ is a diagonal positive definite matrix and

$$\mathrm{sign}(\boldsymbol{s}_1) \triangleq [\,\mathrm{sign}(s_{11}) \quad \cdots \quad \mathrm{sign}(s_{1n})\,]^{\rm T}, \tag{14}$$

with s_{1i} element of $\boldsymbol{s}_1$, $i = 1, \ldots, n$. Alternatively,

$$\dot{\boldsymbol{\sigma}} = \boldsymbol{K}_\beta \boldsymbol{s}_1 + \mathrm{sign}(\boldsymbol{s}_1) \tag{15}$$

can be used.

To analyze the stability of the control approach, it is necessary to define the closed loop dynamics. In order to do so, we carry out the following development.

$$\boldsymbol{s}_{\mathrm{r}} \triangleq \dot{\boldsymbol{q}} - \dot{\boldsymbol{q}}_{\mathrm{r}} = \frac{1}{\alpha_\lambda}\boldsymbol{J}^{-1}(\boldsymbol{q})\boldsymbol{R}_\phi \boldsymbol{s}_{\mathrm{y}} \quad (16)$$

$$\boldsymbol{s}_{\mathrm{y}} \triangleq \dot{\boldsymbol{y}} - \dot{\boldsymbol{y}}_{\mathrm{r}} = \alpha_\lambda \boldsymbol{R}_\phi \boldsymbol{J}(\boldsymbol{q})\boldsymbol{s}_{\mathrm{r}}. \quad (17)$$

Then, one can rewrite (1) as

$$\boldsymbol{H}(\boldsymbol{q})\dot{\boldsymbol{s}}_{\mathrm{r}} + \boldsymbol{C}(\boldsymbol{q},\dot{\boldsymbol{q}})\boldsymbol{s}_{\mathrm{r}} + \boldsymbol{D}\boldsymbol{s}_{\mathrm{r}} = \boldsymbol{\tau} - \boldsymbol{Y}\boldsymbol{\theta}, \quad (18)$$

where

$$\boldsymbol{Y}\boldsymbol{\theta} \triangleq \boldsymbol{H}(\boldsymbol{q})\ddot{\boldsymbol{q}}_{\mathrm{r}} + \boldsymbol{C}(\boldsymbol{q},\dot{\boldsymbol{q}})\dot{\boldsymbol{q}}_{\mathrm{r}} + \boldsymbol{D}\dot{\boldsymbol{q}}_{\mathrm{r}} + \boldsymbol{g}(\boldsymbol{q}) + \boldsymbol{\tau}_{\mathrm{p}}. \quad (19)$$

Yis an $m \times n$ matrix independent of the dynamic parameters, θ is a $m \times 1$ vector of the constants parameters, furthermore $\dot{q}_r$, $\ddot{q}_r$ and $\ddot{y}_r$ are defined as

$$\dot{\boldsymbol{q}}_{\mathrm{r}} \triangleq \frac{1}{\alpha_\lambda}\boldsymbol{J}^{-1}(\boldsymbol{q})\boldsymbol{R}_\phi \dot{\boldsymbol{y}}_{\mathrm{r}} \quad (20)$$

$$\ddot{\boldsymbol{q}}_{\mathrm{r}} = \frac{1}{\alpha_\lambda}\dot{\boldsymbol{J}}^{-1}(\boldsymbol{q})\boldsymbol{R}_\phi \dot{\boldsymbol{y}}_{\mathrm{r}} + \frac{1}{\alpha_\lambda}\boldsymbol{J}^{-1}(\boldsymbol{q})\boldsymbol{R}_\phi \ddot{\boldsymbol{y}}_{\mathrm{r}}, \quad (21)$$

where $\dot{\boldsymbol{J}}^{-1}(\boldsymbol{q}) = \frac{\mathrm{d}}{\mathrm{d}t}\boldsymbol{J}^{-1}(\boldsymbol{q})$.

$$\ddot{\boldsymbol{y}}_{\mathrm{r}} = \ddot{\boldsymbol{y}}_{\mathrm{d}} - \boldsymbol{\Lambda}_{\mathrm{y}}(\dot{\boldsymbol{y}} - \dot{\boldsymbol{y}}_{\mathrm{d}}) - k\boldsymbol{s}_{\mathrm{d}} - \boldsymbol{K}_\gamma \dot{\boldsymbol{\sigma}}, \quad (22)$$

The proposed control law is given by

$$\boldsymbol{\tau} = -\boldsymbol{K}_{\mathrm{p}}\boldsymbol{J}^{\mathrm{T}}(\boldsymbol{q})\boldsymbol{R}_\phi \boldsymbol{s}_{\mathrm{y}} + \boldsymbol{Y}\hat{\boldsymbol{\theta}}, \quad (23)$$

where $\boldsymbol{K}_{\mathrm{p}} \in \mathbb{R}^{2\times 2}$ is a positive definite matrix.

$$\dot{\hat{\boldsymbol{\theta}}} = -\frac{1}{\alpha\lambda}\boldsymbol{\Gamma}\boldsymbol{Y}^T\boldsymbol{J}^{-1}(\boldsymbol{q})\boldsymbol{R}_\phi(\boldsymbol{s}_{\mathrm{y}}), \quad (24)$$

Rewritng the control law as

$$\boldsymbol{\tau} = -\bar{\boldsymbol{K}}_{\mathrm{p}}\left\{\frac{1}{\alpha_\lambda}\boldsymbol{J}^{-1}(\boldsymbol{q})\boldsymbol{R}_\phi \boldsymbol{s}_{\mathrm{y}}\right\} + \boldsymbol{Y}\hat{\boldsymbol{\theta}}. \quad (25)$$

$\bar{\boldsymbol{K}}_{\mathrm{p}} \in \mathbb{R}^{2\times 2}$ has been obtained after some rather direct manipulation and it is defined as

$$\bar{\boldsymbol{K}}_{\mathrm{p}} \triangleq \alpha_\lambda \boldsymbol{K}_{\mathrm{p}}\boldsymbol{J}^{\mathrm{T}}(\boldsymbol{q})\boldsymbol{J}(\boldsymbol{q}), \quad (26)$$

By taking into account (16) one can write (25) as

$$\boldsymbol{\tau} = -\bar{\boldsymbol{K}}_{\mathrm{p}}\boldsymbol{s}_{\mathrm{r}} + \boldsymbol{Y}\hat{\boldsymbol{\theta}}. \quad (27)$$

Then, the tracking error closed loop dynamics is obtained by substituting (27) in (18) to get

$$\boldsymbol{H}(\boldsymbol{q})\dot{\boldsymbol{s}}_{\mathrm{r}} + \boldsymbol{C}(\boldsymbol{q},\dot{\boldsymbol{q}})\boldsymbol{s}_{\mathrm{r}} + \boldsymbol{K}_{\mathrm{DP}}\boldsymbol{s}_{\mathrm{r}} = \boldsymbol{Y}\tilde{\boldsymbol{\theta}} \quad (28)$$

where $\boldsymbol{K}_{\mathrm{DP}} \triangleq \boldsymbol{D} + \bar{\boldsymbol{K}}_{\mathrm{p}}$ and $\tilde{\boldsymbol{\theta}} = \boldsymbol{\theta} - \hat{\boldsymbol{\theta}}$.

Now, a theorem can be established.

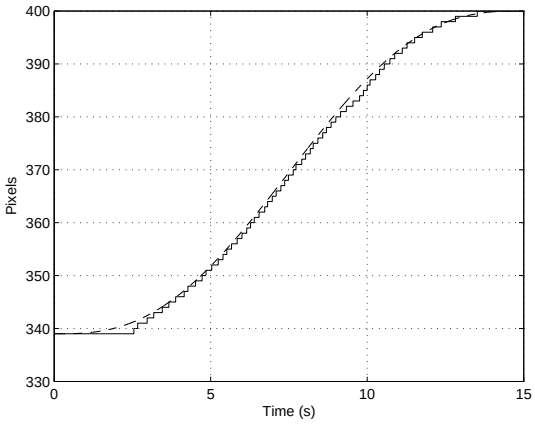

Figura 2. a) y_1 (——), $y_{\mathrm{d}1}$ (- - -).

Theorem 1: Consider the desired trajectory $\boldsymbol{y}_{\mathrm{d}}$ with $\dot{\boldsymbol{y}}_{\mathrm{d}}$ and $\ddot{\boldsymbol{y}}_{\mathrm{d}}$ bounded , and suppose that the initial condition $\boldsymbol{y}(0)$ and the desired final value $\boldsymbol{y}_{\mathrm{f}}$ are chosen far away enough from any singularity. Then, for the control law (23) a proper combination of the gains k, k_{d}, $\boldsymbol{\Lambda}_{\mathrm{y}}$, $\boldsymbol{K}_\beta$, $\boldsymbol{K}_\gamma$ and $\boldsymbol{K}_{\mathrm{p}}$ can always be found so that tracking ($\Delta\dot{\boldsymbol{y}}$, $\Delta\boldsymbol{y}$,) are bounded and tend to zero.

Remark 1: For a planar robot it is in general quite easy to guarantee that $\boldsymbol{y}_{\mathrm{d}}$ will not reached any singularity.

IV. Simulation results

We have carried out some experiments with the model of the manipulator A465 of *CRS Robotics*. It has six degrees of freedom, but we have used only joints 2 and 3 to have a two degrees of freedom planar robot. Also, we employ a model of the*UNIC UF-1000CL* camera fixed so that the optical axis is perpendicular to the robot planar workspace. In order to implement the control law it is necessary to have $\boldsymbol{y}$ available.

We have used the following parameters $k = 1$, $\boldsymbol{K}_{\mathrm{p}} = 0.090\boldsymbol{I}$, $\boldsymbol{\Lambda}_{\mathrm{z}} = 5\boldsymbol{I}$, $\boldsymbol{\Lambda}_{\mathrm{y}} = 30\boldsymbol{I}$, $\boldsymbol{K}_\gamma = 7\boldsymbol{I}$, $\boldsymbol{K}_\beta = 0.25\boldsymbol{I}$, $\alpha = 67567 pixels/m$ and $\lambda = 0.0085m$.

Note that, since no robot model is necessary, control law (23) can be implemented with voltage and not torque as input. In Figure 2 and Figure 3 actual, desired and estimated image coordinates are shown. It can be appreciated that the final position is reached. Since the camera has a rate of 33Hz, this should have been expected because of the discretezation process of the control law (which makes sampling rate too large to tune control parameters better). The tracking errors are shown in Figures 4.In Figure 6 and Figure 7 it can be seen that the output voltage does have a good behavior without saturation.

In the Figure 8 shows the variation of the parameters estimated by the adaptive control

In the Figure 9 shows the path followed by the end–effector in the image coordinates.

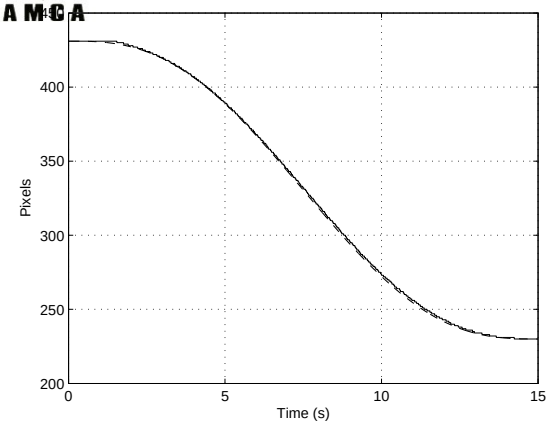

Figura 3. a) y_2 (——), $y_{\mathrm{d}2}$ (- - -).

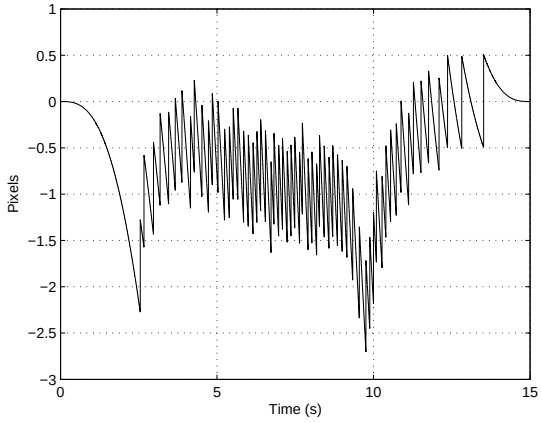

Figura 4. a) Δy_1.

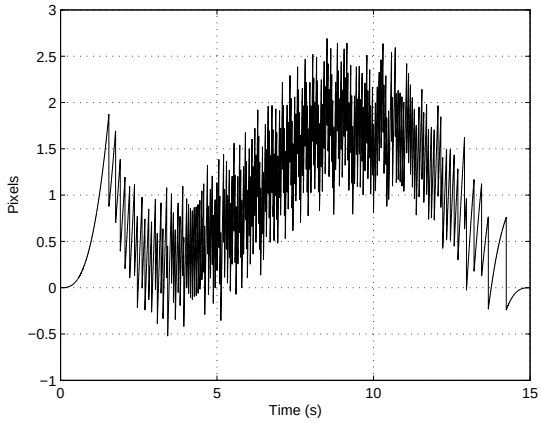

Figura 5. Δy_2.

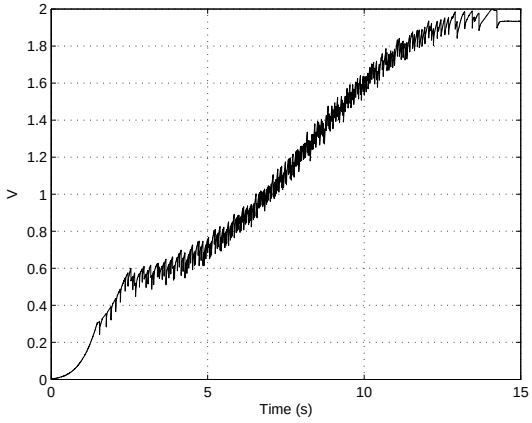

Figura 6. Output voltage V_1.

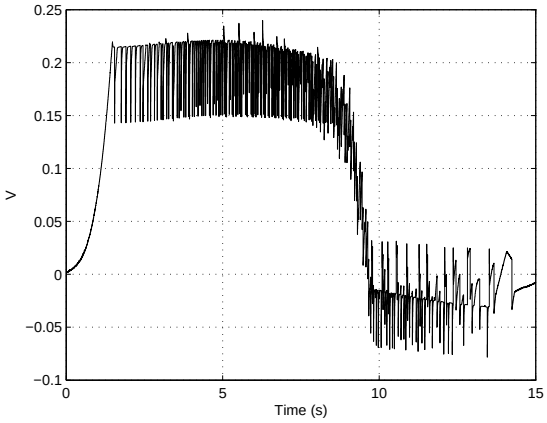

Figura 7. Output voltage V_2.

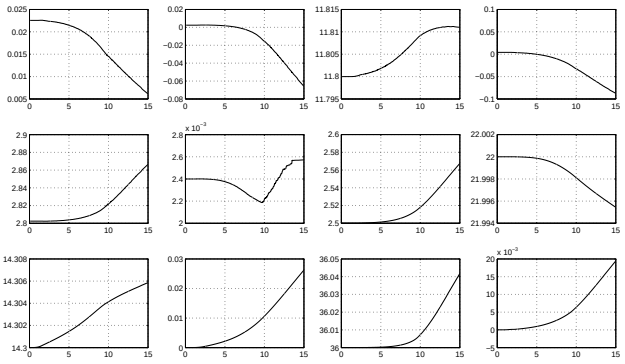

Figura 8. Paramaters Estimated for the Adaptive Control

V. Conclusions

In this paper we present an adaptation of a control algorithm designed to work in Cartesian coordinates to a scheme that employs image coordinates in a visual servoing approach. As a direct consequence, only any parameters of the camera and the robot base frame is required for implementation. To test the theory, simulation results have been carried out which show a good performance of the proposed method.

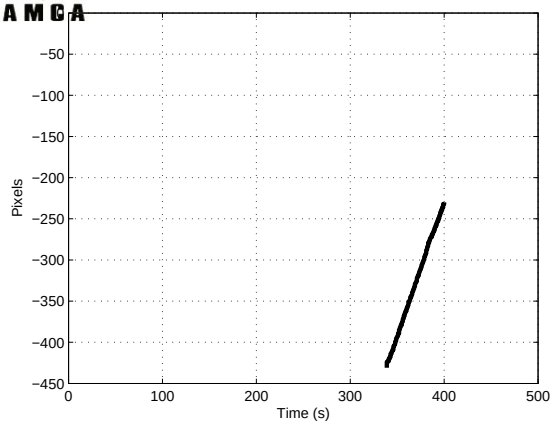

Figura 9. Path in pixels

VI. ACKNOWLEDGMENTS

This work is based on research supported by the **CONACYT** under grant **58112** and by the **DGAPA–UNAM** under grant **IN105408**.

VII. PROOF OF THEOREM 1 1

In this appendix, the proof of Theorem 1 is presented. As we noted in the introduction, this is a modification of the algorithm presented in(Arteaga et al., 2008) with application to visual servoing, so that we just present the main issues of the proof for our current work, while the interested reader can look for details in the reference. Consider the following theorem and lemma.

Theorem 2: (Arteaga et al., 2008) and (Hutchinson et al., 1996) Let $\mathbb{D} \subset \mathbb{R}^n$ be a domain that contains the origin and $V : [0, \infty) \times \mathbb{D} \to \mathbb{R}$ be a continuously differentiable function such that

$$\alpha_1(\|\boldsymbol{x}\|) \leq V(t, \boldsymbol{x}) \quad \leq \quad \alpha_2(\|\boldsymbol{x}\|) \tag{29}$$

$$\frac{\partial V}{\partial t} + \frac{\partial V}{\partial \boldsymbol{x}} \boldsymbol{f}(t, \boldsymbol{x}) \quad \leq \quad -W_3(\boldsymbol{x}), \ \ \forall \ \|\boldsymbol{x}\| \geq \mu > 0 \tag{30}$$

$\forall\ t \geq 0$ and $\forall\ \boldsymbol{x} \in \mathbb{D}$, where α_1 and α_2 are class $\mathcal{K}$ functions, $W_3(\boldsymbol{x})$ is a continuous positive definite function and $\boldsymbol{f} : [0, \infty) \times \mathbb{D} \to \mathbb{R}^n$ is piecewise continuous in t and locally Lipschitz in $\boldsymbol{x}$ on $[0, \infty) \times \mathbb{D}$. Take $r > 0$ such that $\mathbb{B}_{\rm r} = \{\boldsymbol{x} \in \mathbb{R}^n | \|\boldsymbol{x}\| \leq r\} \subset \mathbb{D}$ and suppose that

$$\mu < \alpha_2^{-1}(\alpha_1(r)). \tag{31}$$

Then, there exits a class $\mathcal{KL}$ function β and for every initial state $\boldsymbol{x}(t_0)$, satisfying

$$\|\boldsymbol{x}(t_0)\| \leq \alpha_2^{-1}(\alpha_1(r)), \tag{32}$$

there is $T \geq 0$ (dependent on $\boldsymbol{x}(t_0)$ and μ) such that the solution of $\dot{\boldsymbol{x}} = \boldsymbol{f}(t, \boldsymbol{x})$ satisfies

$$\|\boldsymbol{x}\| \quad \leq \quad \beta(\|\boldsymbol{x}(t_0)\|, t - t_0), \ \ \forall\ t_0 \leq t \leq t_0 + T \tag{33}$$

$$\|\boldsymbol{x}\| \quad \leq \quad \alpha_1^{-1}(\alpha_2(\mu)), \qquad \forall\ t \geq t_0 + T. \tag{34}$$

Moreover, if $\mathbb{D} = \mathbb{R}^n$ and α_1 belongs to class K_∞, then (33)–(34) hold for any initial state $\boldsymbol{x}(t_0)$, with no restriction on how large μ is. △

Lemma 1: (Arteaga et al., 2008) Consider (13)–(14), and suppose you have the relationship

$$\boldsymbol{s}_{\rm i} = \boldsymbol{s}_1 + \boldsymbol{K}_\gamma \boldsymbol{\sigma}. \tag{35}$$

If $\|\boldsymbol{s}_{\rm i}\| \leq \bar{s}_{\rm i} < \infty$ for all time, then $\boldsymbol{\sigma}$ and $\boldsymbol{s}_1$ are bounded for all time. Furthermore, a bound for $\boldsymbol{\sigma}$ is given by

$$\sigma_{\max} = \frac{2\left(\lambda_{\max}(\boldsymbol{K}_\beta)\bar{s}_{\rm i} + \sqrt{n}\right)}{\lambda_{\min}(\boldsymbol{K}_\beta \boldsymbol{K}_\gamma)}. \tag{36}$$

△

As done in (Arteaga et al., 2008), we prove Theorem 1 in three steps.

a) First of all, we show that if $\boldsymbol{x} = [\,\boldsymbol{s}_{\rm r}^{\rm T}\ \theta^T]$ is bounded by $x_{\max}$, then any other signal is bounded. This proceeds as follows. From (9)–(11) and (17) one gets

$$\boldsymbol{s}_{\rm i} = \boldsymbol{s}_1 + \boldsymbol{K}_\gamma \boldsymbol{\sigma}, \tag{37}$$

with $\boldsymbol{s}_{\rm i} \stackrel{\triangle}{=} \boldsymbol{s}_{\rm y}$ bounded. By applying Lemma 1 one concludes that $\boldsymbol{\sigma}$ and $\boldsymbol{s}_1$ are bounded. On the other hand, from (8), (9) and (17) one has

$$\Delta\dot{\boldsymbol{y}} + \boldsymbol{\Lambda}_{\rm y}\Delta\boldsymbol{y} = \boldsymbol{s}_{\rm y} + \boldsymbol{s}_{\rm d} - \boldsymbol{K}_\gamma\boldsymbol{\sigma}. \tag{38}$$

The dynamic equation for $\Delta\boldsymbol{y}$ represents a stable linear filter with bounded input, so that $\Delta\boldsymbol{y}$ and $\Delta\dot{\boldsymbol{y}}$ must be bounded. We can select that both $\boldsymbol{y}_{\rm d}$, $\dot{\boldsymbol{y}}_{\rm d}$ and $\ddot{\boldsymbol{y}}_{\rm d}$are bounded. Then, since $\Delta\boldsymbol{y} = \boldsymbol{y} - \boldsymbol{y}_{\rm d}$, one concludes that $\boldsymbol{y}$ and $\dot{\boldsymbol{y}}$ are also bounded. On the other hand, from (5) it is

$$\dot{\boldsymbol{q}} = \frac{1}{\alpha_\lambda}\boldsymbol{J}^{-1}(\boldsymbol{q})\boldsymbol{R}_\phi\dot{\boldsymbol{y}}. \tag{39}$$

In view of Assumption 1, $\boldsymbol{q}$ must be bounded since no singularity has been reached and $\dot{\boldsymbol{q}}$ is bounded after (39). Now, from (9) $\dot{\boldsymbol{y}}_{\rm r}$ is bounded and so is $\dot{\boldsymbol{q}}_{\rm r}$. Then we compute

$$\ddot{\boldsymbol{y}}_{\rm r} \quad = \quad \ddot{\boldsymbol{y}}_{\rm d} - \boldsymbol{\Lambda}_{\rm y}(\dot{\boldsymbol{y}} - \dot{\boldsymbol{y}}_{\rm d}) - k\boldsymbol{s}_{\rm d} - \boldsymbol{K}_\gamma\dot{\boldsymbol{\sigma}}, \tag{40}$$

which must be bounded because from (15) $\dot{\boldsymbol{\sigma}}$ is bounded. We also have

$$\ddot{\boldsymbol{q}}_{\rm r} = \frac{1}{\alpha_\lambda}\dot{\boldsymbol{J}}^{-1}(\boldsymbol{q})\boldsymbol{R}_\phi\dot{\boldsymbol{y}}_{\rm r} + \frac{1}{\alpha_\lambda}\boldsymbol{J}^{-1}(\boldsymbol{q})\boldsymbol{R}_\phi\ddot{\boldsymbol{y}}_{\rm r}, \tag{41}$$

where $\dot{\boldsymbol{J}}^{-1}(\boldsymbol{q}) = \frac{\rm d}{{\rm d}t}\boldsymbol{J}^{-1}(\boldsymbol{q})$. Then $\ddot{\boldsymbol{q}}_{\rm r}$ is bounded because the boundedness of $\dot{\boldsymbol{q}}$ ensures that of $\dot{\boldsymbol{J}}^{-1}(\boldsymbol{q})$. Also, by taking into account that $\boldsymbol{\tau}_{\rm p}$ is bounded by assumption, $\boldsymbol{Y}\theta$ in (19) is bounded, and so is $\dot{\boldsymbol{s}}_{\rm r}$ after (28).
We also have

$$\dot{\hat{\boldsymbol{\theta}}} = -\frac{1}{\alpha\lambda}\boldsymbol{\Gamma}\boldsymbol{Y}^T\boldsymbol{J}^{-1}(\boldsymbol{q})\boldsymbol{R}_\phi(\boldsymbol{s}_{\rm y}), \tag{42}$$

where, $\dot{\hat{\boldsymbol{\theta}}}$ is bounded and $\boldsymbol{\theta} = \int_0^t \dot{\hat{\boldsymbol{\theta}}}(\vartheta)\mathrm{d}\vartheta + \theta(0)$ is bounded. Note also that from (27) the input torque $\boldsymbol{\tau}$ is bounded, so that from (1) $\ddot{\boldsymbol{q}}$ must be bounded. It is also possible to compute from (5)

$$\ddot{\boldsymbol{y}} = \alpha_\lambda \boldsymbol{R}_\phi \dot{\boldsymbol{J}}(\boldsymbol{q})\dot{\boldsymbol{q}} + \alpha_\lambda \boldsymbol{R}_\phi \boldsymbol{J}(\boldsymbol{q})\ddot{\boldsymbol{q}}, \tag{43}$$

which turns out to be bounded as well. Finally, from (17) one has $\dot{\boldsymbol{s}}_{\rm y} = \ddot{\boldsymbol{y}} - \ddot{\boldsymbol{y}}_{\rm r}$ bounded, so that from (11) and (37) $\dot{\boldsymbol{s}}_{\rm i}$ is bounded too.

b) The next step is to show that, with a proper choice of gains, one can actually achieve $\|\boldsymbol{x}\| \leq x_{\max}$. As done in (Arteaga et al., 2008), we consider for simplicity $x_{\max}$ as a given value. Now define

$$V(\boldsymbol{x}) = \frac{1}{2}\boldsymbol{x}^{\rm T}\boldsymbol{M}\boldsymbol{x}, \tag{44}$$

with $\boldsymbol{M} \triangleq$ block diag $\{\, \boldsymbol{H}(\boldsymbol{q}) \quad \boldsymbol{\Gamma}^{-1} \,\}$. After Property 1 it satisfies

$$\lambda_1\|\boldsymbol{x}\|^2 \leq V(\boldsymbol{x}) \leq \lambda_2\|\boldsymbol{x}\|^2, \tag{45}$$

with

$$\lambda_1 \triangleq \frac{1}{2}\min_{\forall \boldsymbol{q}\in\mathbb{R}^2} \lambda_{\min}(\boldsymbol{M}(\boldsymbol{q})) \tag{46}$$

$$\lambda_2 \triangleq \frac{1}{2}\max_{\forall \boldsymbol{q}\in\mathbb{R}^2} \lambda_{\max}(\boldsymbol{M}(\boldsymbol{q})). \tag{47}$$

Now we use $V(\boldsymbol{x})$ in (44) and Theorem 2, with $\alpha_1 = \lambda_1\|\boldsymbol{x}\|^2$ and $\alpha_2 = \lambda_2\|\boldsymbol{x}\|^2$. By using Property 2, the derivative of V along (28) is given by

$$\begin{aligned}\dot{V} &= -\boldsymbol{s}_{\rm r}^{\rm T}\boldsymbol{K}_{\rm DP}\boldsymbol{s}_{\rm r} - \boldsymbol{s}_{\rm r}^{\rm T}\boldsymbol{Y}\tilde{\boldsymbol{\theta}} + \tilde{\theta}\Gamma^{-1}\dot{\tilde{\theta}} \\ &= -\boldsymbol{s}_{\rm r}^{\rm T}\boldsymbol{K}_{\rm DP}\boldsymbol{s}_{\rm r} + \tilde{\theta}\big[\Gamma^{-1}\dot{\tilde{\theta}} + Y\boldsymbol{s}_{\rm r}\big] \\ &= -\boldsymbol{s}_{\rm r}^{\rm T}\boldsymbol{K}_{\rm DP}\boldsymbol{s}_{\rm r} \leq 0. \end{aligned} \tag{48}$$

Since $V(t)$ is lower bounded by zero and decreases for any nonzero $\mathbf{s}_{\rm r}$, as seen from 48, it seen plausible from the above equation that $\dot{V}(t)$, and therefore the tracking error measure $\mathbf{s}_{\rm r}$, must converge to zero.

c) Till now we have shown that $\boldsymbol{x}$ is bounded. We still have to prove that tracking and observation errors tend to zero. This can be done exactly as developed in item c) of the proof given in (Arteaga et al., 2008).

REFERENCES

S. Hutchinson, G. D. Hager, and P. I. Corke. (1996). *A tutorial on visual servo control*. IEEE Transactions on Robotics and Automation, vol. 12, pp. 651-670.

R. Kelly and F. Reyes. 2000. *On vision systems identification with application to fixedcamera robotic systems*.International Journal of Imaging Systems and Technology, vol. 11, no. 3, pp. 170-180.

E. C. Dean-Leon, V. Parra-Vega, and A. Espinosa-Romero. (2006). *Global uncalibrated visual servoing for constrained robots working on an uncalibrated environment*. IEEE/RSJ International Conference on Intelligent Robots and Systems, Beijing, China, October , pp. 3809-3816.

R. R. Perez, M. A. Arteaga-Prez, R. Kelly, and A. Espinosa. (2008). *On output regulation of direct visual servoing via velocity fields* . International Journal of Control, Vol. 82, no. 4, pp. 679-688.

L. Sciavicco and B. Siciliano. (2000). *Modeling and Control of Robot Manipulators*. 2nd ed. London, Great Britain: SpringerVerlag, 2000.

Jean J. Slotine and W. Li. (1988). *Adaptive Manipulator Control: A Case Study)*. IEEE Transactiosn On Automatic Control, vol 33, no. 11, pp.995-1003.

D. Dawnson, L. Lewis and C. Abdallah. (2004). *Robot Manipulator Control. Theory and Practice)*. 2nd ed. Marcel Dekker, New Yersey, 2004.

R. Kelly, J. Moreno, and R. Campa,. (2004). *Visual servoing of planar robots via velocity fields)*. 43rd IEEE Conference on Decision and Control, pp.4028-4033.